CFD Letters

Journal homepage:
https://semarakilmu.com.my/journals/index.php/CFD_Letters/index
ISSN: 2180-1363

CFD Analysis and Development of Mixing Tank Design for the Fermented Starch Production Process

Sigit Purwanto[1,*], Bayu Novariawan[1], Suparman[2], Palupi Tri Widiyanti[3], Isnaini Pratiwiningrum[4], Fitri Nur Kayati[5]

[1] Research Center for Process and Manufacturing Industry Technology, National Research and Innovation Agency (BRIN), Indonesia
[2] Research Center for Agroindustry, National Research and Innovation Agency (BRIN), Indonesia
[3] Laboratory for Fuel and Design Engineering, National Research and Innovation Agency (BRIN), Indonesia
[4] Advanced Characterization Laboratories, National Research and Innovation Agency (BRIN), Indonesia
[5] Bureau of Organization and Human Resources, National Research and Innovation Agency (BRIN), Indonesia

ARTICLE INFO

Article history:
Received 14 March 2023
Received in revised form 20 April 2023
Accepted 25 May 2023
Available online 5 December 2023

Keywords:
Stirred fermenter tank; CFD; impeller; power reduction

ABSTRACT

Stirred tanks are widely used in the industrial world, design and improvements are still being developed, including the stirred fermenter tank. A numerical study was carried out to examine the relationship between experimental and reference and computational analysis, in order to minimize the power consumption of a stirred fermenter tanks and optimize the velocity distribution and its profile in radial and axial direction. Specifically, velocity distribution profile in radial and axial direction and the profile of pressure distribution of an experimental impeller, a flat impeller, and a flat-hole impeller were investigated using Computational Fluid Dynamic (CFD) analysis. It was found that the axial velocity at the top and the bottom of the experimental impeller was highly disparate at around 0.95 m/s, while the flat impeller and the flat-hole impeller experienced a disparity of 0.05 m/s and 0.21 m/s, respectively. In case terms of decreased power, the experimental impeller showed power reduction of 21%, greater than that of the flat-hole impeller configuration of 17%.

1. Introduction

The mixing process using a stirred tank is widely developed in the processing industry. The important challenges in this application are mixing performance, impeller tip velocity, and efficient energy input [1]. A Mixing of dissolved solids is needed to increase the interaction between particles, so that uneven accumulation at one point can be avoided [2]. The mixing flow in a stirred tank creates a flow that is difficult to predict, so it is necessary to pay attention to the selection of equipment to produce sufficient turbulence and flow [3]. In addition, mixing fluids in large-scale industries using impellers may generate flow movements with high turbulence.

A mixing process using impeller is also applied in Tapioca Pilot Plant with a capacity of 5 tons tapioca per day belonged to the Starch Laboratory – the National Research and Innovation Agency

* *Corresponding author.*
E-mail address: sigi011@brin.go.id (Sigit Purwanto)

https://doi.org/10.37934/cfdl.16.1.95106

Republic of Indonesia (BRIN). This facility combines modern and conventional technology to produce native and fermented starch [4]. In case of fermented starch, a development of fermentation process was carried out by changing the process design from settling tanks to a fermenter tank. The fundamental problem of fermentation using a settling tank is the inhomogeneity of suspense concentration and mixing process, and also the considerable chance of contamination. These may be solved by a fermenter tank that is able to maintain the hygienic surroundings and the homogeneity of the fermented suspense.

This project aimed to analyze the fluid flow systems inside the fermented tank using Computational Fluid Dynamics (CFD) and improve the performance over more applicable technology. Three different types of impellers, i.e., experimental impeller, flat impeller, and flat-hole impeller, were investigated and modeled in a stirred fermenter tank using commercial software ANSYS Fluent 2021 R2. Then, experimental testing was carried out as a validation of the modeling results. This article presents a study of the velocity profiles in the radial and axial directions and the pressure distribution in three impeller configurations.

2. Methodology

2.1 Design Calculation of Fermenter Tank

The experiment of design development for fermenter tank was one part of the modification process of tapioca flour production. This process involved the activity of microorganism (i.e lactic acid bacteria) to create acidic surroundings with a pH of around 4. Therefore, a well-mixing process between tapioca slurry and the bacteria was targeted to avoid inhomogeneity, so that the desired result could be achieved. This was facilitated by a fermenter tank equipped with two impellers that placed at different level of the stirring rod, with configuration showed in Table 1.

Table 1
The experimental data of the fermenter

Item of experimental data	Description
Impeller Type	Disc Turbine, 3 blade at 45^o angle
Operating Conditions	25°C, 1 atm
Tank Diameter (D_t)	2.75 m = 9.0223 ft
Tank height (Z_R)	3 m = 9.8425 ft
Distance from bottom of the tank to stirrer (Z_i)	0.15 m = 0.4921 ft
Tank volume (V)	17.8259 m^3
Tapioca slurry volume (Z_L=2,4m)	2.4 m = 14,260. m^3
Tapioca Density (ρ)	1,173.15 kg/m^3
Tapioca viscosity (μ)	3.000 cP
Stirrer diameter (D_i)	≈2/3D_t (1.8m= 3.2808 ft)
Dt /D_i	1.52 m
Z_L /D_i	1.33 m
Z_i /D_i	0.083 m

The fermenter tank is in the form of a vertical cylinder vessel, with a diameter of Dt = 2.75 m supported by four legs. There are no baffles in the tank because the principle of the process is to mix native starch with water to obtain homogeneity as a form of starch slurry. The distance between the upper and lower impellers, Zp (Z_R/2) is 1.5 m. While the distance between the bottom of the tank and the position of the lower impeller is Zi/Di= 0.083 m. The shape and scheme of the fermenter tank is shown in Figure 1.

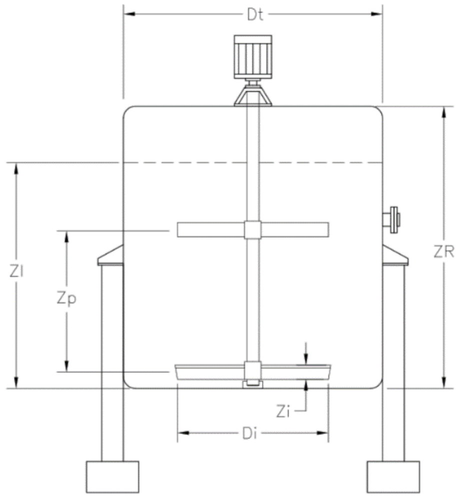

Fig. 1. Fermenter tank design

The stirrer in the fermenter tank was a paddle type, with its blade number determined by Rase [5]:

$$\mathrm{n} = \frac{WELH}{ID} \tag{1}$$

Where, WELH (Water Equivalent Liquid High) = Z_L x sg; since sg (the specific gravity) of tapioca is 1.1173; then WELH is calculated as 2.8156 m = 9.2374 ft. While ID = D_t is the inside diameter of the stirrer (m), hence the number of blades (n) =2-3, and then it was determined to be 3 blades. The rotational speed of the stirrer in the fermenter tank is calculated by Rase [5] as follows:

$$\mathrm{N} = \frac{600}{\pi . Di} . \sqrt{\frac{WELH}{2. Di}} \tag{2}$$

It brought the speed (N) of 69.04 rpm, and was set to be 69 rpm. While the condition of the fluid can be assessed by the Reynolds number. For Newtonian fluids, the Reynolds number is defined as follows:

$$\mathrm{Re} = \frac{n . \rho . Di^2}{\mu} \tag{3}$$

Where ρ is the fluid density (kg/m^3), n is the impeller speed (rpm), D_i s the agitator diameter (m), and μ is the fluid dynamic viscosity (kg/ms). In this experiment, the working fluid of slurry starch was used, that has ρ = 1,173.15 kg/m^3 and μ = 3,000 cP.

2.2 Geometry of Fermenter Tank

This study investigated a fermenter tank equipped with two impellers placed at different level of the stirring rod, each impeller consisting of 3 blades. The design of the fermenter tank was based on results of design and experiments conducted in previous work [4]. The fermenter tank modeling was executed on three types of impellers, with the same tank size and blade, namely fermenter diameter (D_t) = 2.75 m, fermenter height (Z_R) = 3 m, and the distance between the upper and lower impellers, Z_m = 1.5 m. While the dimension of the blade was 1 m x 0.15 m, and the height of the fermented starch liquid was 2.4 m. In the first configuration, the experimental impeller had a bottom impeller with a tilt angle of 45^o and top impeller with 90^o upright. The second configuration used a flat type impeller with the bottom and top 90^o upright. Meanwhile, the third configuration applied a flat-hole type of impeller with the bottom and top is 90^o upright and had a hole on each blade with dimensions of 0.2 m x 0.04 m. These three configurations are shown in Figure 2.

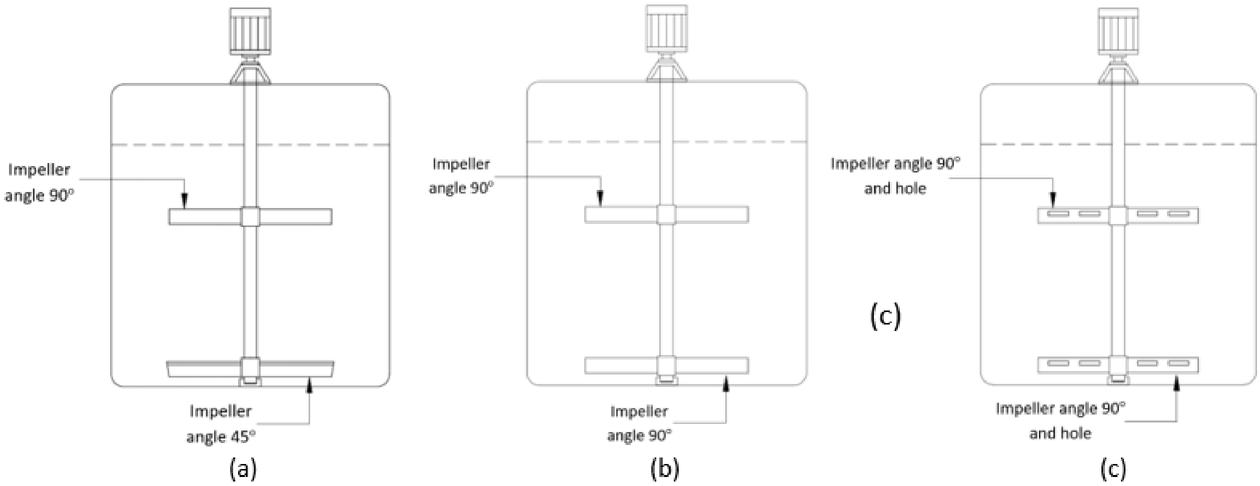

Fig. 2. Impeller type configuration (a) experimental impeller (b) flat impeller and (c) flat-hole impeller

2.3 Governing Equation

In this study, the Navier-Stokes equation was used to solve the calculation of the fluid flow pattern in the fermenter tank. Calculations were solved with continuity and momentum equations, for Newtonian fluids with constant density and velocity. The continuity equation was used to describe the flow in the x, y, and z directions [6].

Continuity:

$$\frac{\partial}{\partial x}(\rho u) + \frac{\partial}{\partial y}(\rho v) + \frac{\partial}{\partial z}(\rho w) = 0 \tag{4}$$

x-momentum:

$$\rho g_x - \frac{\partial P}{\partial x} + \mu\left(\frac{\partial^2 u}{\partial x^2} + \frac{\partial^2 u}{\partial y^2} + \frac{\partial^2 u}{\partial z^2}\right) = \rho\frac{du}{dt} \tag{5}$$

y-momentum:

$$\rho g_y - \frac{\partial P}{\partial y} + \mu\left(\frac{\partial^2 v}{\partial x^2} + \frac{\partial^2 v}{\partial y^2} + \frac{\partial^2 v}{\partial z^2}\right) = \rho\frac{dv}{dt} \tag{6}$$

z-momentum:

$$\rho g_z - \frac{\partial P}{\partial x} + \mu\left(\frac{\partial^2 w}{\partial x^2} + \frac{\partial^2 w}{\partial y^2} + \frac{\partial^2 w}{\partial z^2}\right) = \rho\frac{dw}{dt} \quad (7)$$

Where $u, v, and\ w$ are the velocity components in the $x, y, and\ z$ directions; ρ is density; μ is viscosity; t is time; and P is pressure.

2.4 Turbulence Models

A realizable $k-\varepsilon$ model is used to calculate the fluid turbulence model in the fermenter tank. A realizable $k-\varepsilon$ mathematical model considers the relationship of the Boussinesq equation and the definition of eddy viscosity [7, 8]. The advantage of this approach is the relatively low computational cost. The Boussinesq hypothesis for predicting isotropic turbulent viscosity usually work well for shear flows dominated by only one turbulent shear stress. Realizable $k-\varepsilon$ models have better predictions when realized for boundary layer characteristics in large pressure gradients, segregated flows, and circulations [9, 10].

The Boussinesq hypothesis method relates the Reynolds stress to the mean velocity gradient, as follow:

$$-\rho\overline{u_i' u u_j'} = \mu_t\left(\frac{\partial u_i}{\partial x_j} + \frac{\partial u_j}{\partial x_i}\right) - \frac{2}{3}\left(\rho k + \mu_t\frac{\partial u_k}{\partial x_k}\right)\delta_{ij} \quad (8)$$

The turbulent viscosity, μ_t , is defined as

$$\mu_t = \rho C_\mu \frac{k^2}{\varepsilon} \quad (9)$$

Where C_μ is a constant.

Transport equations for Realizable models $k-\varepsilon$ is :

$$\frac{\partial}{\partial t}(\rho k) + \frac{\partial}{\partial x_j}(\rho k u_j) = \frac{\partial}{\partial x_j}\left[\left(\mu + \frac{\mu_t}{\sigma_k}\right)\frac{\partial k}{\partial x_j}\right] + G_k + G_b - \rho\varepsilon - Y_M + S_k \quad (10)$$

$$\frac{\partial}{\partial t}(\rho\varepsilon) + \frac{\partial}{\partial x_j}(\rho\varepsilon u_j) = \frac{\partial}{\partial x_j}\left[\left(\mu + \frac{\mu_t}{\sigma_\varepsilon}\right)\frac{\partial\varepsilon}{\partial x_j}\right] + \rho C_1 S\varepsilon - \rho C_2\frac{\varepsilon^2}{k + \sqrt{v \in}} + C_{1\varepsilon\frac{\varepsilon}{k}} C_{3\varepsilon} G_b + S_\varepsilon \quad (11)$$

And

$$C_1 = max\left[0.43\frac{\eta}{\eta + 5}\right], \eta = S\frac{k}{\varepsilon}, S = \sqrt{2S_{ij}S_{ij}} \quad (11)$$

In this equation, G_k represents the generation of turbulence kinetic energy due to the mean velocity gradients. G_b is the generation of turbulence kinetic energy due to buoyancy. Y_M represents the contribution of the fluctuating dilatation in compressible turbulence. C_1 and $C_{1\varepsilon}$ are constants. σ_k and σ_ε are the turbulent Prandtl numbers for k and ε, respectively. S_k and $S\varepsilon$ are user-defined source terms. The model constant value is $C_{1\varepsilon} = 1.44, C_{2\varepsilon} = 1.92, C_\mu = 0.09$, $\sigma_k = 1.0$, $\sigma_\varepsilon = 1.3$ [7].

2.5 Computational Methodology

This study used the Ansys Fluent 2021R2 solver to solve the flow equation in the stirred tank modelling. The flow domain utilized a 3-zone MRF (Multiple Reference Frame) approaches, namely the main domain, and two moving domains consisting of lower impeller domain and upper impeller domain. The boundary condition of the tank wall was defined as a "no slip" condition. Meanwhile, at the top of the tank, specified shear conditions were applied because it was considered that the fluid does not reach the top of the tank [11]. The boundary conditions set for a stirred tank are shown in Figure 3. The working material was tapioca slurry with an experimental density of ρ = 1,173 kg/m^3 and viscosity of μ = 3,000 cP. In all simulation sections, the time step was determined as a function of the impeller speed, which was 69 rpm. The mesh used was polyhedral with high mesh quality (skewness = 0.90) ensured throughout the domain, as shown in Figure 4.

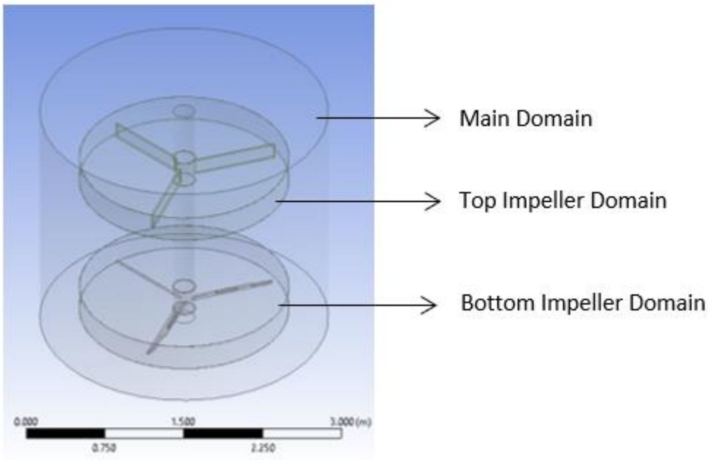

Fig. 3. Boundary conditions adopted for CFD model

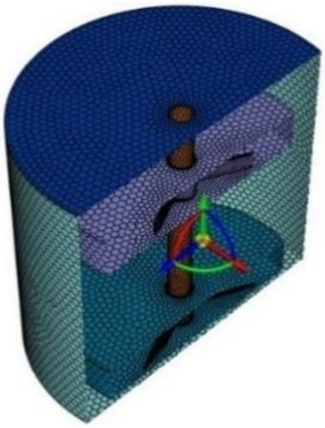

Fig. 4. Meshing for the CFD section of the fermenter tank model

3. Results and Discussions

3.1 Distribution of Velocity

Figure 5 shows the distribution of flow patterns for stirred fermenter tanks equipped with different impeller shapes and positions. An overview of the flow patterns in the three types of impellers created four recirculation zones, extending near the tank walls. The flow pattern was formed at the bottom and top of each impeller. The velocity distribution showed a changing flow pattern from the impeller surface to the tank wall. The results showed that the experimental impeller, a recirculation flow pattern occurred closer to the impeller, than the flat impeller and flat-hole impeller. This was because the lower impeller of the experimental configuration had a tilt angle of 45°. The results of the experimental simulation of recirculating flow patterns in positions below and above the impeller are in accordance with those reported by other researchers [12]. Impellers in the top and bottom position were required to reduce the weak flow zone in a stirred fermenter tank. The intensity of the turbulence was characterized by the formed flow pattern, i.e., the flat hole impeller had a more intense number of direction changes than the experimental impeller and flat impeller. The occurrence of flow patterns that have varying intensities according to the results of experimental simulations have been reported by other researchers [13]. Moreover, the velocity along the fermenter tank wall is zero, because this area is a no-slip condition [14].

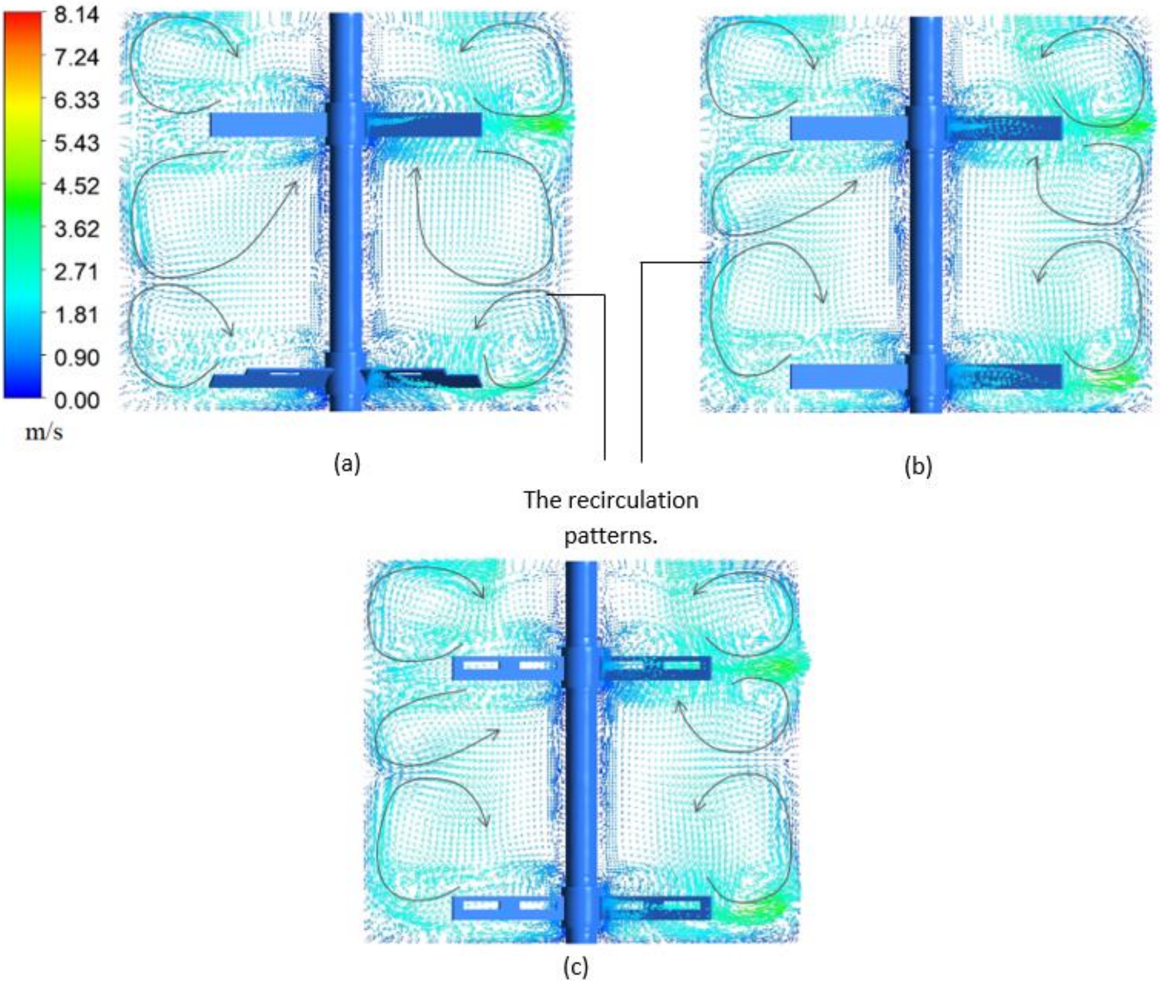

Fig. 5. Velocity distribution for three impeller configurations (a) Experimental impeller (b) Flat impeller and (c) Flat-hole impeller

3.2 Speed Profile in Radial and Axial Directions

Figure 6 provides a comparison of velocity profiles in a stirred fermenter tank. The highest radial velocity was concentrated at the impeller tip in all three configurations. Impellers with an upright type affected the size of the mixed fluid area and had a strong radial flow pattern. This was due to the higher surface interaction of the impeller structure with the fluid [15-17]. Velocity contour profiles of the three types of impeller configurations at two radial locations were z = 0.2 m and 1.75 m.

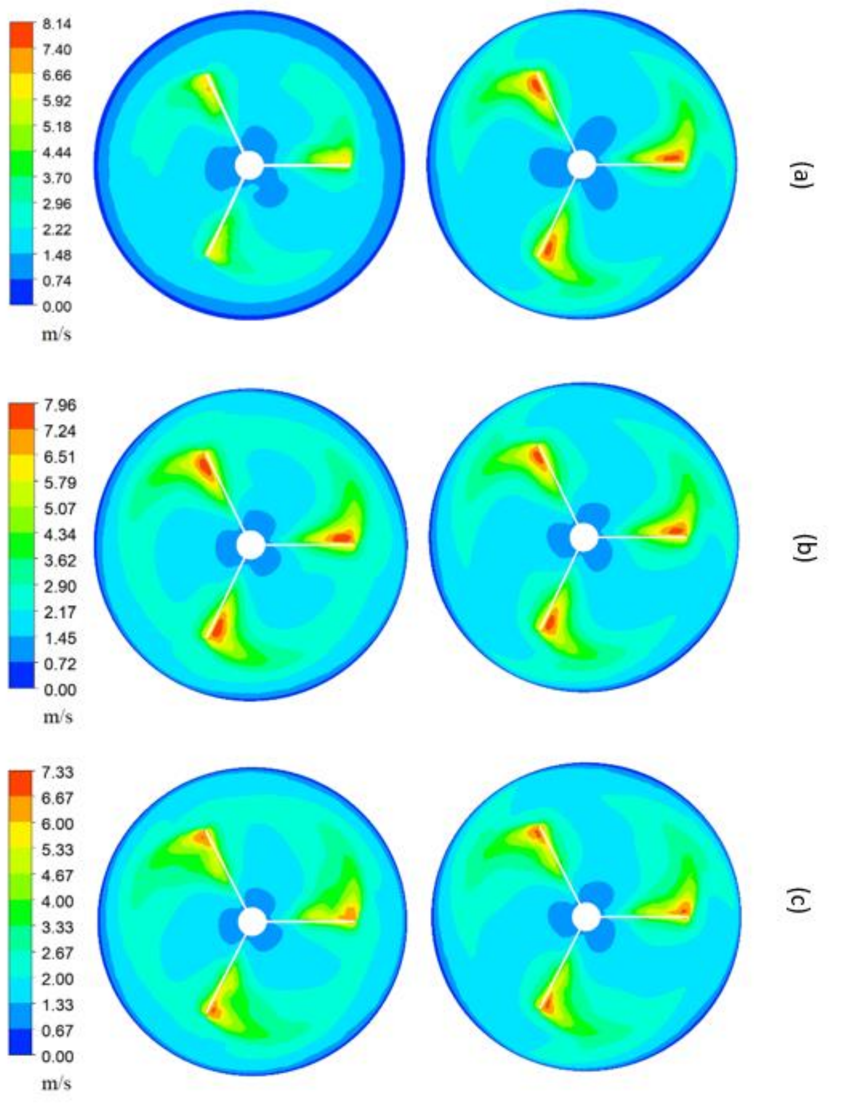

Fig. 6. Speed contour in the radial direction with three impeller configurations (a) Experimental impeller (b) Flat impeller and (c) Flat-hole impeller

Figure 7 reveals that the modeling results obtained the axial velocity values of the impeller experimental configuration at the bottom and top were 1.78 m/s and 2.73 m/s. Meanwhile, the axial velocity on the flat impeller was 2.00 m/s and 2.05 m/s and the axial velocity on the impeller flat hole were 1.93 m/s and 2.14 m/s. The three configurations formed patterns that were similar at their corresponding axial direction points (z = 0.2 m and 1.75 m). The axial velocity with a maximum value occurred at a location near the impeller, then it decreased at the positions above and below the impeller. This axial velocity profile of an impeller simulation is also observed by other research reports namely [18, 19], who reported the results of research on impeller simulations with axial velocity profiles.

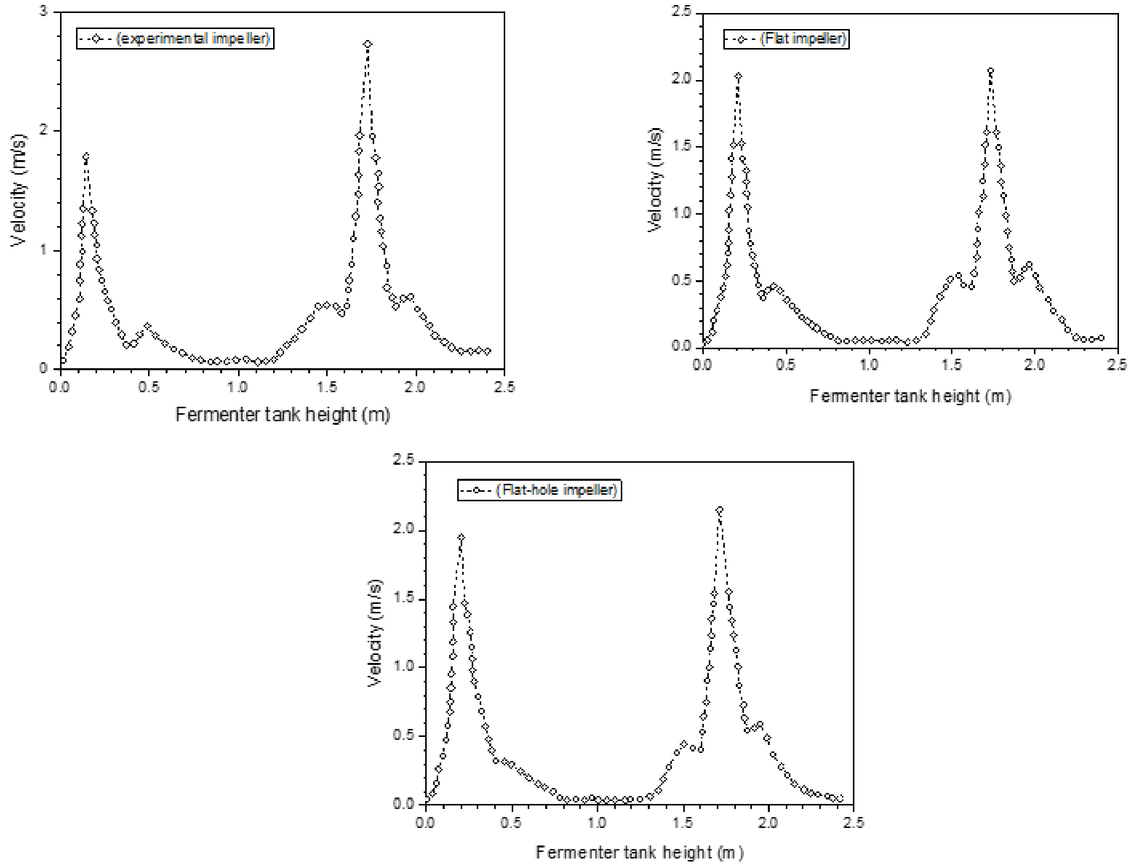

Fig. 7. The velocity profile in the axial direction with three impeller configurations

3.3 Pressure Distribution Profile

Figure 8 indicates the influence of the pressure distribution that occurs on the impeller surface. The rear impeller surface experienced negative pressure, while the front impeller surface exhibited the highest positive pressure. This happened to all three types of impeller configurations. The pressure distribution is also reported in research by Hoseini *et al.,* [13]. Lower pressure took place on the experimental impeller and flat hole impeller, while the pressure was higher on the flat impeller type. The results of the three impellers were described as a function of the moment in the stirred fermenter tank.

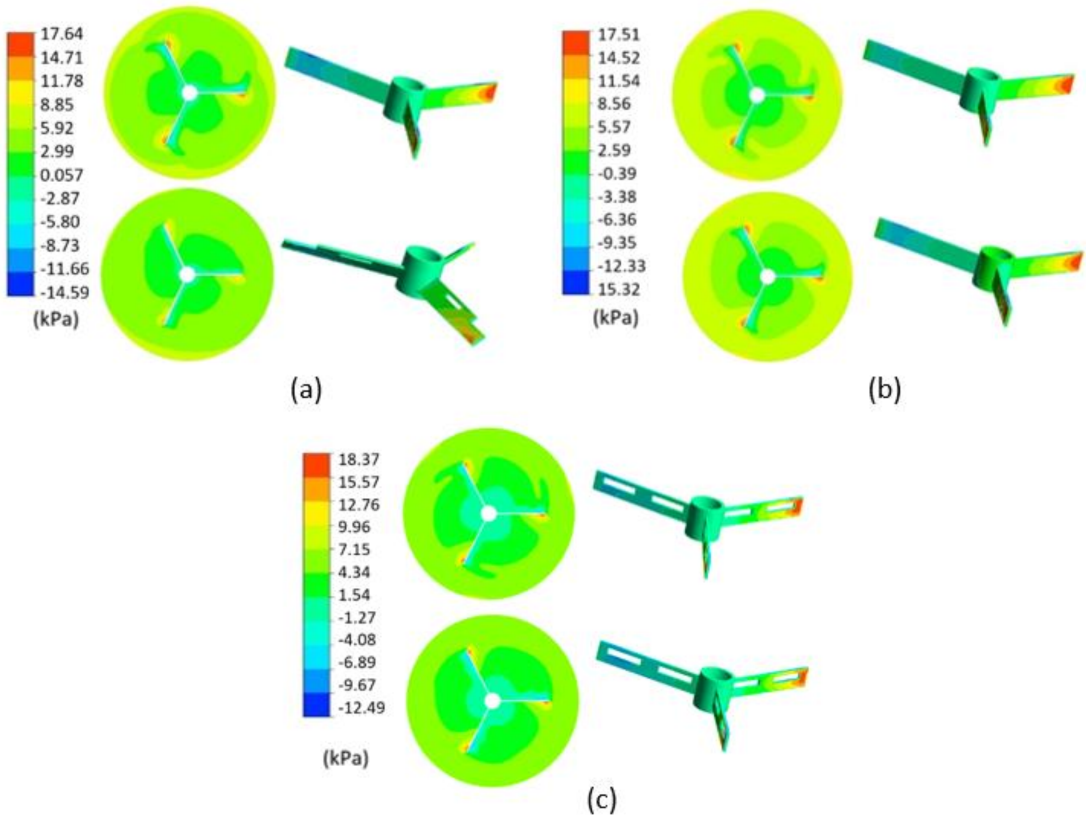

Fig. 8. Pressure distribution with three impeller configurations (a) Experimental impeller (b) Flat impeller and (c) Flat-hole impeller

3.4 Power Consumption

The experimental process of a stirred fermenter tank was done to test the ability of the impeller so that it could function properly (see Figure 9). The first experiment was carried out using an electric motor with a power of 1.5 kW with a starch slurry level of 0.75 m. When operating for 2-3 hours the electric motor burned out, so modifications were executed to the impeller to reduce the load during the stirring process. This was performed by reducing length of the impeller and changing the angle of inclination of the bottom impeller by 45°. Then the second experiment was carried out using an electric motor with a power of 5.5 kW with a starch slurry level of 0.75 m. The experimental results showed that the fermenter tank impeller could function to homogeneously mix the starch slurry.

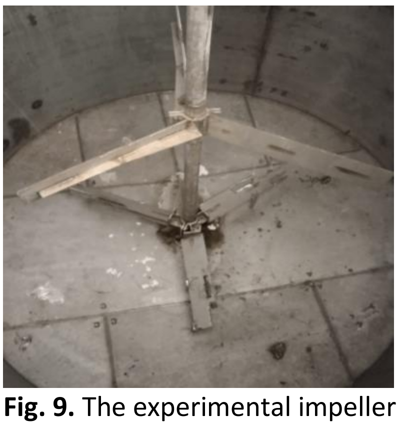

Fig. 9. The experimental impeller

The investigation via modeling of stirred fermenter tank with a maximum starch slurry level of 2.4 m showed that the motor power requirement of the experimental impeller, the flat impeller, and the flat-hole impeller were 24.77, 31.47, and 25.88 kW, respectively (see Figure 10). This indicated that the configuration of the flat impeller had a higher torque than the experimental impeller and the flat hole impeller. Impeller that has no hollow and tilt angle might cause the motor power to be higher by 6.7 kW. Based on this modeling, an impeller modification is one alternative to do, thereby reducing the motor power in the fermenter tank, hence obtaining an efficient and proper motor power. Alternative modifications could be made by making a hole in the impeller section or changing the position of the impeller to an angle of 45°. Meanwhile, the impeller with a 45° angle of inclination has no significant effect on torque reduction.

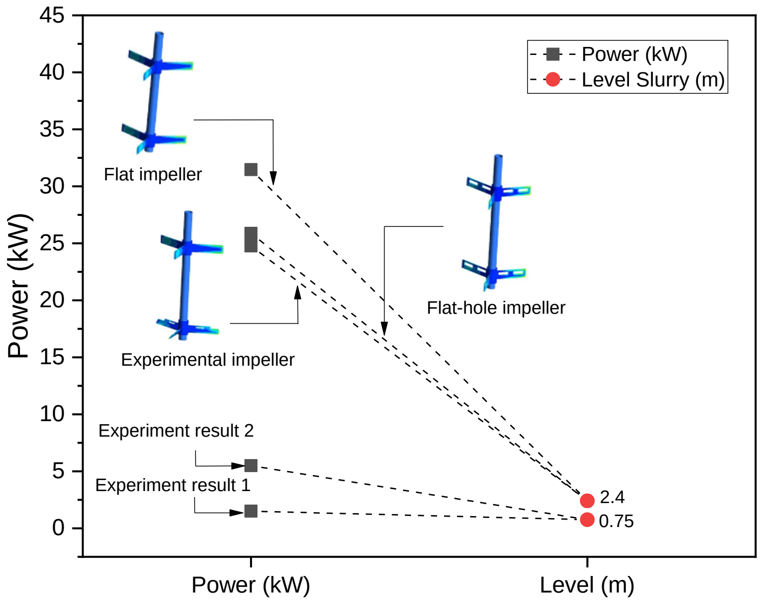

Fig. 10. Power consumption in a stirred fermenter tank

4. Conclusions

The characterization of fluid mixing using a stirred tank with 3 impeller configurations was investigated using CFD simulations and experimental analysis. Distribution of velocity, velocity profile in radial and axial directions, pressure distribution profile, and power consumption were analyzed through CFD with a realizable $k-\varepsilon$ model approach. The results showed that the experimental impeller with an angle of 45° at the bottom stirrer created a recirculation flow pattern closer to the impeller than that of the flat impeller and the flat-hole impeller. In terms of the impeller axial velocity, the velocity disparity between the bottom and the top stirrer of the experimental impeller, flat impeller, and flat-hole impeller were calculated for 0.95 m/s, 0.05 m/s, and 0.21 m/s, respectively. In terms of power, the experimental impeller showed the greatest power reduction compared to that of the flat hole impeller and the flat impeller, by 21% and 17%. Therefore, modification of the impeller is an alternative means to reduce power consumption while at the same time maintaining stirring the starch slurry at the maximum level.

Acknowledgment
This work was supported by the Starch Technology Laboratory and the Aerodynamics, Aeroelastic and Aeroacoustic Technology Laboratory, National Research and Innovation Agency Republic of Indonesia.

References

[1] Fitschen, Jürgen, Marc Maly, Annika Rosseburg, Johannes Wutz, Thomas Wucherpfennig, and Michael Schlüter. "Influence of spacing of multiple impellers on power input in an industrial-scale aerated stirred tank reactor." *Chemie Ingenieur Technik* 91, no. 12 (2019): 1794-1801. https://doi.org/10.1002/cite.201900121

[2] Mak, Andrew Tsz-Chung. "Solid-liquid mixing in mechanically agitated vessels." University of London, University College London (United Kingdom) (1992).

[3] Torotwa, Ian, and Changying Ji. "A study of the mixing performance of different impeller designs in stirred vessels using computational fluid dynamics." *Designs* 2, no. 1 (2018): 10.https://doi.org/10.3390/designs2010010

[4] Yulianto, Aton, Palupi Tri Widiyanti, *et al.,* "Fermented Starch: Production Testing of Process Stabilization." *Food Science and Nutrition Studies* 3 (1): 1. (2019). https://doi.org/10.22158/fsns.v3n1p1

[5] Rase, H.F. *Chemical Reactor Design for Process Plant*. 1st ed. New York: McGraw Hill Book Company, Inc. (1977).

[6] Patil, Harshal, Ajey Kumar Patel, Harish J. Pant, and A. Venu Vinod. "CFD simulation model for mixing tank using multiple reference frame (MRF) impeller rotation." *ISH Journal of Hydraulic Engineering* 27, no. 2 (2021): 200-209.https://doi.org/10.1080/09715010.2018.1535921

[7] Fluent, A. "ANSYS Fluent Theory Guide ANSYS Inc., Canonsburg, PA. 2020, USA: ANSYS."

[8] Shekhar, S. Murthy, and S. Jayanti. "CFD study of power and mixing time for paddle mixing in unbaffled vessels." *Chemical Engineering Research and Design* 80, no. 5 (2002): 482-498.https://doi.org/10.1205/026387602320224067

[9] Shaheed, Rawaa, Abdolmajid Mohammadian, and Hossein Kheirkhah Gildeh. "A comparison of standard k–ε and realizable k–ε turbulence models in curved and confluent channels." *Environmental Fluid Mechanics* 19 (2019): 543-568. https://doi.org/10.1007/s10652-018-9637-1

[10] Phumnok, Ekaroek, *et al.,* "Study of Hydrodynamics and Upscaling of Immiscible Fluid Stirred Tank using Computational Fluid Dynamics Simulation." *CFD Letters* 14.6 (2022): 115-133. https://doi.org/10.37934/cfdl.14.6.115133

[11] Baba, Ahmad Faiq, Nor Afzanizam Samiran, Razlin Abd Rashid, Izuan Amin Ishak, Zuliazura Mohd Salleh, Rais Hanizam Madon, and Muhammad Suhail Sahul Hamid. "Effect of Impeller's Blade Number on The Performance of Mixing Flow in Stirred Tank using CFD Simulation Method." *CFD Letters* 14, no. 5 (2022): 33-42. https://doi.org/10.37934/cfdl.14.5.3342

[12] Driss, Zied, Sarhan Karray, Wajdi Chtourou, Hedi Kchaou, and M. Salah Abid. "A study of mixing structure in stirred tanks equipped with multiple four-blade Rushton impellers." *Archive of Mechanical Engineering* 59, no. 1 (2012): 53-72.https://doi.org/10.2478/v10180-012-0004-3

[13] Hoseini, S. S., G. Najafi, B. Ghobadian, and A. H. Akbarzadeh. "Impeller shape-optimization of stirred-tank reactor: CFD and fluid structure interaction analyses." *Chemical Engineering Journal* 413 (2021): 127497. https://doi.org/10.1016/j.cej.2020.127497

[14] Perivilli, Satish, Steven Walfish, Erika Stippler, and Mark R. Liddell. "Impact of select geometric and operational parameters on hydrodynamics in dissolution apparatus 2 (paddle apparatus): A design of experiments analysis based on computational fluid dynamics simulations." *Pharmaceutical Research* 39, no. 5 (2022): 919-934.https://doi.org/10.1007/s11095-022-03272-4

[15] Ameur, H. "Energy efficiency of different impellers in stirred tank reactors." *Energy* 93 (2015): 1980-1988. https://doi.org/10.1016/j.energy.2015.10.084

[16] Wang, Shiji, Peng Wang, Jianping Yuan, Jinfeng Liu, Qiaorui Si, and Dun Li. "Simulation Analysis of Power Consumption and Mixing Time of Pseudoplastic Non-Newtonian Fluids with a Propeller Agitator." *Energies* 15, no. 13 (2022): 4561. https://doi.org/10.3390/en15134561

[17] Ameur, Houari, Youcef Kamla, and Djamel Sahel. "Data on the agitation of a viscous Newtonian fluid by radial impellers in a cylindrical tank." *Data in brief* 15 (2017): 752-756. https://doi.org/10.1016/j.dib.2017.10.035

[18] Wu, Mei, Nico Jurtz, Astrid Walle, and Matthias Kraume. "Evaluation and application of efficient CFD-based methods for the multi-objective optimization of stirred tanks." *Chemical Engineering Science* 263 (2022): 118109.https://doi.org/10.1016/j.ces.2022.118109

[19] Gu, Deyin, Hui Xu, Mei Ye, and Li Wen. "Design of impeller blades for intensification on fluid mixing process in a stirred tank." *Journal of the Taiwan Institute of Chemical Engineers* 138 (2022): 104475. https://doi.org/10.1016/j.jtice.2022.104475